AIChE

A Multiperiod Nonlinear Programming Approach for Operation of Air Separation Plants with Variable Power Pricing

Yu Zhu, Sean Legg, and Carl D. Laird
Artie McFerrin Dept. of Chemical Engineering, Texas A&M University, College Station, TX 77843

DOI 10.1002/aic.12464
Published online November 29, 2010 in Wiley Online Library (wileyonlinelibrary.com).

Cryogenic air separation processes consume a large amount of electricity producing significant quantities of high purity gases. Rather than operating at a fixed steady state, it may be profitable to switch among different operating conditions because of variability of electrical prices and product demands. This article addresses the problem of determining the optimal daily multiperiod operating conditions for an air separation process under variable electricity pricing and uncertain product demands. The multiperiod nonlinear programming formulation includes a rigorous nonlinear model of the highly-coupled process, and decision variables include the operating conditions within each period, as well as the transition times. Demand uncertainty is treated using the loss function included in the objective function and constraints on customer satisfaction levels. Solutions are obtained with high computational efficiency, allowing management to make informed decisions regarding operating strategies while considering the trade off between profitability and customer satisfaction levels. © 2010 American Institute of Chemical Engineers *AIChE J,* 57: 2421–2430, 2011
Keywords: optimization, mathematical modeling, gas purification, process simulation, numerical solutions

Introduction

Cryogenic air separation systems are widely utilized for providing significant quantities of high purity nitrogen, argon, and oxygen products in many industries including the steel, chemical, refining, semiconductor, and aeronautical industries. However, cryogenic air separation is an energy-intensive process consuming large amounts of electricity to compress air for separation and liquefying gas products. The industrial gas industry consumed approximately 31,460 million kilowatt hours (over $ 700 million/year) in the USA in 1998, which accounts 3.5% of the total electricity purchased by the manufacturing industry.[1,2] In 2002, the industrial gas industry consumed ~ 35,000 million kilowatt hours of electricity in the USA,[3] which is an increase of 11.3% compared with the amount in 1998. Furthermore, electricity prices are variable and typically follow a daily pattern related to peak/off-peak usage. Because of this variability in power pricing, it may be beneficial to switch among different operating conditions in the pursuit of lowering operating cost while maintaining satisfaction of customer demands. In addition to variable power pricing, optimal operation of air separation systems is affected by market uncertainties (including product prices and demands). These uncertainties are classified and their impact on conceptual design and operation is discussed in Zhu et al.[4]

Previously, Ierapetritou et al.[5] adopted a two stage stochastic programming approach to seek optimal operating strategies under varying power prices. Three different operating modes are defined and a mixed-integer linear

Correspondence concerning this article should be addressed to C. D. Laird at carl.laird@tamu.edu.

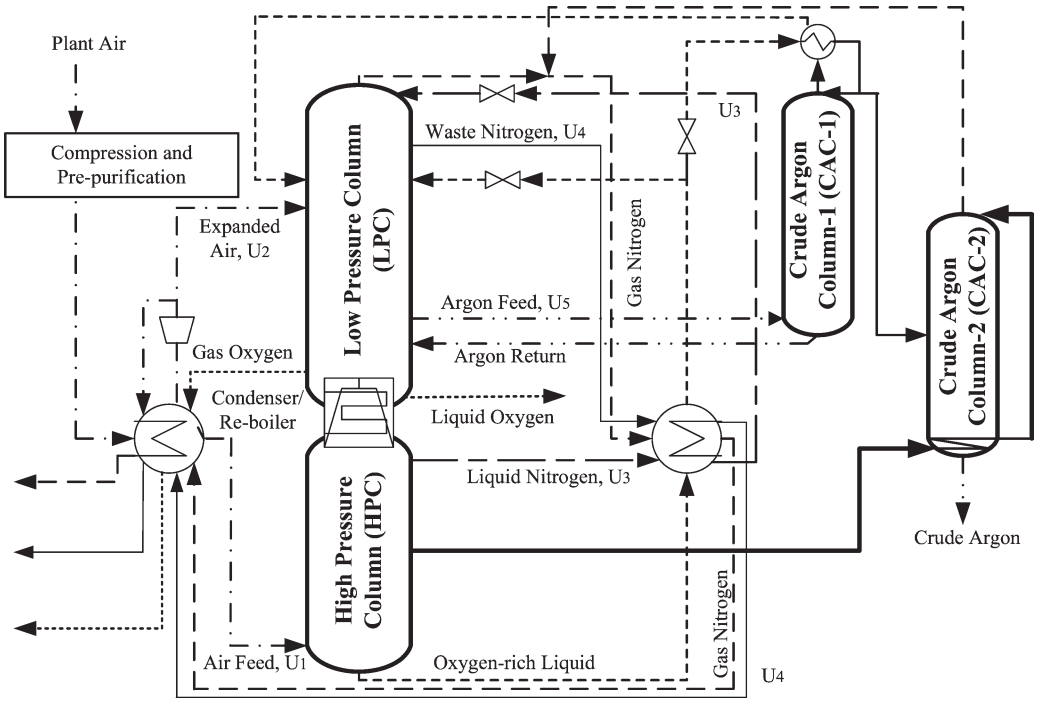

Figure 1. Simplified flowsheet for the cryogenic air separation process.

programming formulation is used to solve for the optimal operating schedule by transitioning among these three modes. Karwan and Keblis[2] developed a similar mixed-integer programming formulation to obtain operating strategies under real time pricing, considering the impact of the forecast horizon length on operating cost. Miller et al.[6] used ideal thermodynamic work to analyze operating strategies under peak and off-peak power prices. The ratio of peak and off-peak power prices is used to determine when intermittent operation of air separation systems is economically feasible. The above research contributions assume instantaneous switching among different operating conditions and typically adopt a simplified or linearized model to capture the process behavior of the complex air separation plant. When changing operation conditions, interactions among several highly-coupled distillation columns and other chemical units must be considered along with safety limits. Therefore, it is preferable to use rigorous nonlinear models that can capture this interaction and reduce plant-model mismatch. In previous work,[7] we developed a nonlinear programming formulation and solution approach to determine optimal operating strategies that considered uncertain demands with probabilistic constraints for contractual obligations. While this work demonstrated that rigorous nonlinear models of the air separation process could be included within this probabilistic optimization formulation, it also assumed that the switching time between different operating conditions was instantaneous. Furthermore, it assumed that electricity prices were constant across the operating cycle.

This article extends previous research and addresses the problem of determining an optimal 24-hour multiperiod operating strategy considering varying power prices, uncertain product demands, and nonzero transition times. The optimization is performed using a rigorous model of an air separation process based on first principles. This model includes the double-effect columns (coupled high and low pressure columns), as well as two crude argon columns for providing high purity argon. Focusing on multiperiod operation, a single day is separated into four different time periods based on the peak/off-peak power prices, and the rigorous nonlinear process model is included within each period. A typical air separation process can take over several hours to reach desired product purities following a complete shutdown. In practice, it is not reasonable to assume instantaneous transition between different operating conditions. Instead, this article assumes a linear relationship between the required load change and the transition time.

In addition to power pricing variability, a probabilistic approach is used in this article to handle uncertain demand requirements from customers. Multiscenario formulations are widely used to deal with uncertainty in design and operation. However, this method typically requires feasibility of each scenario, regardless of scenario probability. Furthermore, the problem size can grow prohibitively large as the number of scenarios is increased. As in our previous work, we have adopted the loss function developed in Li et al.[8] and Nahmias[9] to quantify the expected profit in terms of production rates and uncertain customer demands. To model contractual obligations, a Type 2 service level, as described in Li et al.[8] and Nahmias,[9] is assumed, and the fill-rate expression is used to constrain customer satisfaction levels. This treatment allows decision makers to quantify the interaction between demand uncertainty levels and fill-rate constraints.

The article is organized as follows. First, the cryogenic air separation system under study is described with the rigorous

nonlinear mathematical model of the process and the operational constraints. The multiperiod problem formulation is introduced, and the peak/off-peak pricing schedule used in the case studies is described along with the expressions relating the switching time to the required load changes. Two sets of case studies are presented. The first assumes that the product demands are constant and known. These case studies compare the optimal multiperiod solution with the optimal solution assuming a fixed steady state over the entire horizon. The second set of case studies extends the formulation to include treatment of uncertain product demands. Uncertainty is considered in both the objective function and in customer satisfaction constraints, and results are presented with different levels of uncertainty.

Cryogenic Air Separation Process Model

Figure 1 shows a diagram of the multicolumn separation system under study. Double-effect distillation columns, that is, coupled low and high pressure columns, are a common component of all low temperature cryogenic air separation systems. Crude argon columns (CAC-1 and CAC-2) are often adopted for production of very valuable argon and are included in this case study. Due to addition of the CAC-1 and the CAC-2, significant mass and energy integration is introduced into the process. Therefore, air separation systems with crude argon columns are much more difficult to model and operate than those without. The crude air feed stream is compressed and primary impurities, such as water and carbon dioxide, are removed. After being cooled by a primary heat exchanger, a portion of the air feed stream, called expanded air, is introduced into the low-pressure distillation column (LPC) which contains 70 stages. The remaining feed air stream enters the bottom of the high-pressure distillation column (HPC), which has 36 stages. In the combined condenser/reboiler, the nitrogen vapor stream from the top of the HPC is condensed to produce the reflux for the HPC, while the partially liquefied stream from the bottom of the LPC is vaporized. The liquid nitrogen stream from the top of the HPC is introduced into the top of the LPC, and serves as the reflux stream for the LPC. A portion of the oxygen-rich liquid from the bottom of the HPC is introduced into the 17th tray of the LPC to produce high purity oxygen product. The rest of the oxygen-rich liquid is used by the condenser at the top of the CAC-1 to condense the argon-rich stream and produce the reflux for the CAC-1. A side vapor stream, primarily composed of oxygen and argon, is withdrawn at the 28th tray of the LPC and distilled in the CAC-1. The liquid from the bottom of the CAC-1 is returned to the LPC at the location of vapor stream withdrawal. The crude argon stream enters into the CAC-2 as feed flow. The reboiler at the bottom of the CAC-2 column is heated by the side-stream from the HPC. Oxygen product is taken directly from the bottom of the LPC. Nitrogen product is taken directly from the top of the LPC. Crude argon product is obtained at the bottom of the CAC-2. Column pressures and product specifications for the air separation system under study are listed in the Table 1.

Table 1. Column Pressures and Product Specifications

Oxygen product output, kmol/h	1306
Oxygen product purity	$\geq$ 98%
Nitrogen product purity	$\geq$ 99.99%
Argon product purity	$\geq$ 97
Pressure of LPC, MPa	0.13–0.14
Pressure of HPC, MPa	0.68–0.69
Pressure of CAC-1, MPa	0.12–0.13
Pressure of CAC-2, MPa	0.13–0.14

Distillation Column Model

The four cryogenic distillation columns (LPC, HPC, CAC-1, and CAC-2) are modeled using the tray-by-tray equations including rigorous mass and energy balances, physical properties, and phase equilibrium. The activity coefficient method is used to describe the vapor-liquid equilibrium (VLE) associated with temperature, pressure, and concentrations. Three assumptions for the distillation column models used in this study include: (1) negligible heat loss in the tray; (2) constant pressure drop on each tray; (3) uniform pressure and temperature on each tray. The equations for each tray are given by,

$$0 = V_{j+1}y_{i,j+1} + L_{j-1}x_{i,j-1} + F_j^V z_{i,j}^V + F_j^L z_{i,j}^L - \left(V_j + S_j^V\right)y_{i,j} - \left(L_j + S_j^L\right)x_{i,j} \quad (1)$$

$$0 = V_{j+1}H_{j+1}^V + L_{j-1}H_{j-1}^L + F_j^V H_j^{FV} + F_j^L H_j^{FL} - \left(V_j + S_j^V\right)H_j^V - \left(L_j + S_j^L\right)H_j^L \quad (2)$$

$$H_j^V = \sum_{i\in\mathcal{P}} y_{i,j}\underline{H}_{i,j}^V(T_j,P_j) + \Delta H_{mix}^V(T_j,P_j) \quad (3)$$

$$H_j^L = \sum_{i\in\mathcal{P}} x_{i,j}\underline{H}_{i,j}^L(T_j,P_j) + \Delta H_{mix}^L(T_j,P_j) \quad (4)$$

$$H_j^{FV} = \sum_{i\in\mathcal{P}} y_{i,j}\underline{H}_{i,j}^{FV}\left(T_j^F,P_j^F\right) + \Delta H_{mix}^{FV}\left(T_j^F,P_j^F\right) \quad (5)$$

$$H_j^{FL} = \sum_{i\in\mathcal{P}} x_{i,j}\underline{H}_{i,j}^{FL}\left(T_j^F,P_j^F\right) + \Delta H_{mix}^{FL}\left(T_j^F,P_j^F\right) \quad (6)$$

$$1 = \sum_{i\in\mathcal{P}} y_{i,j} \quad (7)$$

$$y_{i,j} = \gamma_j K_{i,j}x_{i,j} \quad (8)$$

$$K_{i,j} = \exp\left[A_i - \left(B_i/\left(T_j + C_i\right)\right)\right]/P_j \quad (9)$$

$$\log\gamma_{1,j} = \left(\frac{A_{1,3}x_{3,j}^2 + A_{1,2}x_{2,j}^2 + \left(A_{1,3} + A_{1,2} - A_{2,3}\right)x_{3,j}x_{2,j}}{RT_j}\right) \quad (10)$$

$$\log\gamma_{2,j} = \left(\frac{A_{1,2}x_{1,j}^2 + A_{2,3}x_{3,j}^2 + \left(A_{1,2} + A_{2,3} - A_{1,3}\right)x_{1,j}x_{3,j}}{RT_j}\right) \quad (11)$$

$$\log \gamma_{3,j} = \left(\frac{A_{1,3} x_{1,j}^2 + A_{2,3} x_{2,j}^2 + (A_{1,3} + A_{2,3} - A_{1,2}) x_{1,j} x_{2,j}}{RT_j} \right) \tag{12}$$

where j is the index of each tray beginning at the top of each column. F_j^{V} and F_j^{L} are the vapor and liquid molar feed flows entering into the jth tray. S_j^{V} and S_j^{L} are the vapor and liquid molar side flows out of the jth tray. The vapor and liquid flow rates are given by V_j and L_j, respectively. The liquid and vapor compositions are given by $x_{i,j}$ and $y_{i,j}$, respectively. $z_{i,j}^{\mathrm{V}}$ and $z_{i,j}^{\mathrm{L}}$ are the vapor and liquid compositions of feed flows entering into the jth tray. H_j^{FV} and H_j^{FL} are the vapor and liquid enthalpies of feed flows entering into the the jth tray. The vapor and liquid enthalpies of the jth tray are given by H_j^{V} and H_j^{L}, respectively. $\underline{H}_{i,j}^{\mathrm{FV}}$, $\underline{H}_{i,j}^{\mathrm{FL}}$, $\underline{H}_{i,j}^{\mathrm{V}}$ and $\underline{H}_{i,j}^{\mathrm{L}}$ are the vapor and liquid enthalpies of each pure component in the feed flow and each tray, respectively. The enthalpies of mixing, ΔH_{mix}, are described with a polynomial regressed against system data over the relevant process conditions. R is the ideal gas constant. The Margules constants, $a_{i,k}$, describe the liquid phase interactions between components i and k. Margules constants can be found in Harmens,[10] while Antoine constants are reported in http://webbook.nist.gov/chemistry/.

As a result of abnormal operation, significant quantities of nitrogen may enter the crude argon column. Nitrogen, being the most volatile of the components, will concentrate at the top of column and form a noncondensable mixture, disrupting the column operation as shown in Baukal.[11] Therefore, the nitrogen purity in the feed flow from LPC to CAC-1 must be constrained, and the following inequalities are added for the feed flow from the LPC to the CAC-1.[11,12]

$$z_{N_2,LPC-CAC1}^{V} \leq 0.001 \tag{13}$$

$$0.08 \leq z_{Ar,LPC-CAC1}^{V} \leq 0.10 \tag{14}$$

$$0.90 \leq z_{O_2,LPC-CAC1}^{V} \leq 091. \tag{15}$$

Heat Transfer Equations

Heat exchanger models are expressed by their mass and energy balances, while all throttle valves are assumed to be isenthalpic throttle processes. The energy, Q_1, is transferred within the combined condenser/reboiler, which is assumed to be an additional normal tray for both the HPC and the LPC. This energy is extracted from the condensing vapor stream at the top of the HPC and is released into the vaporizing liquid stream at the bottom of the LPC. Similarly, the condenser of the CAC-1 is heat integrated with the oxygen-rich stream from the bottom of the HPC. The relevant energy, Q_2, is transferred in the condenser of the CAC-1. This energy is extracted from the condensing vapor stream at the top of the CAC-1 and released into a portion of oxygen-rich liquid stream from the HPC. This stream is partially vaporized. The reboiler of the CAC-2 is heat integrated with the outlet stream from the HPC. The relevant energy, Q_3, is transferred in the reboiler of the CAC-2. This energy is extracted from the outlet stream of the HPC and released for boiling up the liquid flow in the bottom of the CAC-2. These heat transfer expressions are given by,

$$Q_1 = UA_1 \left(T_1^{HPC} - T_{70}^{LPC} \right) \tag{16}$$

$$Q_2 = UA_2 \left(T_1^{CAC-1} - T_{O_2-\mathrm{rich}}^{HPC} \right) \tag{17}$$

$$Q_3 = UA_3 \left(T_{10}^{HPC} - T_{41}^{CAC-2} \right) \tag{18}$$

where UA_1, UA_2, and UA_3 are the heat transfer coefficients in the condenser/reboiler, the top of the CAC-1, and the bottom of the CAC-2, respectively. Here, they are equal to 23480, 7727, and 6520 (W/K). T_1^{HPC} is the temperature in the first tray of the HPC and T_{70}^{LPC} is the temperature in the last tray of the LPC. $T_1^{\mathrm{CAC-1}}$ is the temperature of the first tray of the CAC and $T_{O_2-\mathrm{rich}}^{\mathrm{HPC}}$ is the temperature of the oxygen-rich liquid stream from the bottom of the HPC. T_{10}^{HPC} is the temperature in the 10th tray of the HPC and $T_{41}^{\mathrm{CAC-2}}$ is the temperature in the last tray of the CAC-2.

Liquifier and Compressor Work

Products from an air separation plant may be available as both a gas and a liquid. All liquids in our process are liquefied gas products. Therefore, the dominant operating cost is the energy consumed by the air compressors and liquefiers. We assume the pressure drop through pipelines, throttle valves, heat exchangers, and other units are constant during the transient operation. The main air compressor is an integral gear centrifugal compressor. Assuming an adiabatic compression process, the work is given by,

$$W_n^{\mathrm{C}} = \frac{\Phi_n^{\mathrm{F}}}{1 - \Delta V_{\mathrm{loss}}} \frac{\kappa}{\kappa - 1} RT_n^{\mathrm{C}} \left[\left(\frac{P_{\mathrm{out}}^{\mathrm{C}}}{P_{\mathrm{in}}^{\mathrm{C}}} \right)^{\left(\frac{\kappa-1}{\kappa}\right)} - 1 \right] \eta_1^{-1}, \tag{19}$$

where adiabatic index number of gas, κ, and compression efficiency, η_1, are 1.4 and 0.686, respectively. Φ_n^{F} is the total amount of air feed flow into the air separation system during the nth period. $P_{\mathrm{in}}^{\mathrm{C}}$ and $P_{\mathrm{out}}^{\mathrm{C}}$ are the entering and exiting flow pressures of the compressor. The flow loss ratio of the air compressor, ΔV_{loss}, is 0.04. The liquefier consists of a makeup compressor and a recycle system including the warm and cold expanders.

The liquefier work is given by,

$$W_n^{\mathrm{L}} = \left(\sum_{i \in \mathcal{P}} V_{i,n}^{\mathrm{L}} \Delta H_{i,n}^{\mathrm{L}} \right) \eta_2^{-1} \tag{20}$$

where the liquifier efficiency $\eta_2 = 0.5$, and $\mathcal{P}$ is the set of products, namely nitrogen, argon, and oxygen. $V_{i,n}^{\mathrm{L}}$ and $\Delta H_{i,n}^{\mathrm{L}}$ are liquefied product flows and corresponding enthalpy changes, respectively.

Multiperiod Problem Formulation

In this section, we develop a multiperiod formulation that allows for different steady state operating conditions within

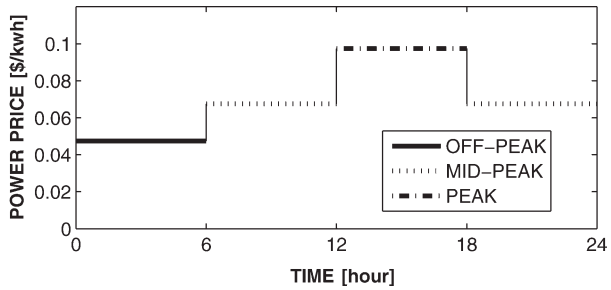

Figure 2. Four periods of daily operation associated with peak/off-peak power pricing.

each period. Variability of power prices is one of the main reasons for switching between different operating conditions. The example pricing schedule used in the case studies is shown in Figure 2. In the multiperiod formulation, the daily operation of the air separation process is separated into four periods according to this schedule. In our case studies, the peak, off-peak, and mid-peak prices are assumed to be 0.0974, 0.0474, and 0.0674 $/kWh. $T^{\mathrm{M}} = [0,6,12,18]$ are the time points between consecutive periods. Note that the time period could easily be reduced to smaller units such as 1h if the resolution of the power pricing or other inputs warrant. Unequal intervals can be also formulated in our approach, by changing the values of T^{M}.

Equations 1–20, coupled with the mass and energy balances for all recycle streams and piping equipment form the rigorous, steady state model for the air separation process. These equations are included in the multiperiod formulation as constraints describing the process model for each period n. In this work, we do not consider the possibility of shutting down the crude argon columns since the process may require very long periods of time to recover normal argon production in the event of a shutdown. Other practical issues need to be considered when switching between different operating conditions. These factors include the operating range of the compressor, pressure control in the distillation columns, and performance of the expanders. Therefore, to prevent hazardous risks like compressor surge, large pressure ramps, and nitrogen block in the crude argon columns, we do not assume instantaneous transition, but rather restrict the rate of transition between periods. Here, we assume a linear relationship between the transition time and the change in the air feed flow rate. Furthermore, we allow the start time of the transition to be an optimization variable. It is assumed that increasing the load values from 65 to 115% requires 126 min, while decreasing the load values from 115 to 65% also requires the same 126 min, giving a transition slope of 0.4%/min. The air feed flow rate in period n is defined by V_n^{A}. $\bar{V}_n^{\mathrm{A}}$ is the feed flow rate at the start of the nth period (i.e. at time T_n^{M} during the transition). V_n^{A} and $\bar{V}_n^{\mathrm{A}}$ are given by,

$$V_n^A = U_{1,n} + U_{2,n},\ n \in (1,2,3,4) \tag{21}$$

$$\bar{V}_n^{\mathrm{A}} = V_n^{\mathrm{A}} - b_n\left(T_n^{\mathrm{F}} - T_n^{\mathrm{M}}\right),\ n \in (1,2,3,4) \tag{22}$$

where b_n represents the transition slope defined previously. T_n^{F} is the final time of the transition into time period n, while T_n^{S} is the start time of the transition out of time period n. Their relationship is defined by,

$$T_1^F = T_4^S + \frac{\left(V_1^A - V_4^A\right)}{b_1} - 24 \tag{23}$$

$$T_n^F = T_{n-1}^S + \frac{\left(V_n^A - V_{n-1}^A\right)}{b_n}, n \in (2,3,4) \tag{24}$$

$$T_n^M \le T_n^F \le T_n^S \le T_{n+1}^M, n \in (1,2,3,4). \tag{25}$$

The variables relating to the transition are all described in Figure 3. The value of the slope b_n is positive if the process is transitioning from a period of low feed flow rate to a period of high feed flow rate, and negative for the opposite case. Note that the transition from positive slope to negative slope is smooth since it occurs when the difference between V_n^{A} and V_{n-1}^{A} (and hence the transition time) is zero. The total amount of air feed flow compressed in each period, Φ_n^{F}, is described by,

$$\Phi_n^{\mathrm{F}} = \frac{1}{2}\left(V_n^{\mathrm{A}} + \bar{V}_n^{\mathrm{A}}\right)\left(T_n^{\mathrm{F}} - T_n^{\mathrm{M}}\right) + V_n^{\mathrm{A}}\left(T_n^{\mathrm{S}} - T_n^{\mathrm{F}}\right) + \tfrac{1}{2}\left(V_n^{\mathrm{A}} + \bar{V}_{n+1}^{\mathrm{A}}\right)\left(T_{n+1}^{\mathrm{M}} - T_n^{\mathrm{S}}\right), n \in (1,2,3) \tag{26}$$

$$\Phi_4^{\mathrm{F}} = \frac{1}{2}\left(V_4^{\mathrm{A}} + \bar{V}_4^{\mathrm{A}}\right)\left(T_4^{\mathrm{F}} - T_4^{\mathrm{M}}\right) + V_4^{\mathrm{A}}\left(T_4^{\mathrm{S}} - T_4^{\mathrm{F}}\right) + \tfrac{1}{2}\left(V_4^{\mathrm{A}} + \bar{V}_1^{\mathrm{A}}\right)\left(T_1^{\mathrm{M}} - T_4^{\mathrm{S}}\right). \tag{27}$$

Similarly, the total amount of each liquefied product at the nth period, $\Phi_{i,n}^{\mathrm{L}}$, is given by,

$$\Phi_{i,n}^{\mathrm{L}} = \frac{1}{2}\left(S_{i,n}^{\mathrm{P}} + \bar{S}_{i,n}^{\mathrm{P}}\right)\left(T_n^{\mathrm{F}} - T_n^{\mathrm{M}}\right) + S_{i,n}^{\mathrm{P}}\left(T_n^{\mathrm{S}} - T_n^{\mathrm{F}}\right) + \tfrac{1}{2}\left(S_{i,n}^{\mathrm{P}} + \bar{S}_{i,n+1}^{\mathrm{P}}\right)\left(T_{n+1}^{\mathrm{M}} - T_n^{\mathrm{S}}\right), i \in \mathcal{P}, n \in (1,2,3) \tag{28}$$

$$\Phi_{i,4}^{\mathrm{L}} = \frac{1}{2}\left(S_{i,4}^{\mathrm{P}} + \bar{S}_{i,4}^{\mathrm{P}}\right)\left(T_4^{\mathrm{F}} - T_4^{\mathrm{M}}\right) + S_{i,4}^{\mathrm{P}}\left(T_4^{\mathrm{S}} - T_4^{\mathrm{F}}\right) + \tfrac{1}{2}\left(S_{i,4}^{\mathrm{P}} + \bar{S}_{i,1}^{\mathrm{P}}\right)\left(T_1^{\mathrm{M}} - T_4^{\mathrm{S}}\right), i \in \mathcal{P} \tag{29}$$

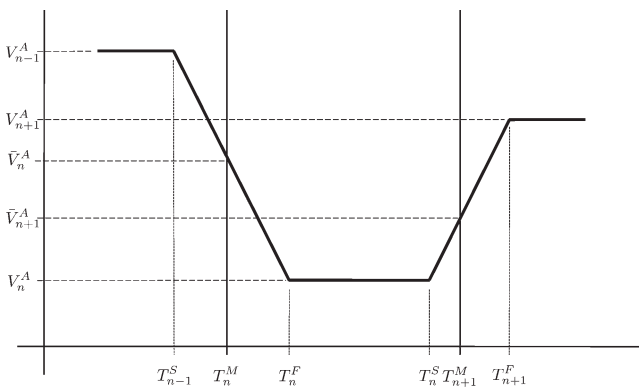

Figure 3. Variable definitions for air feed flow load change during transition.

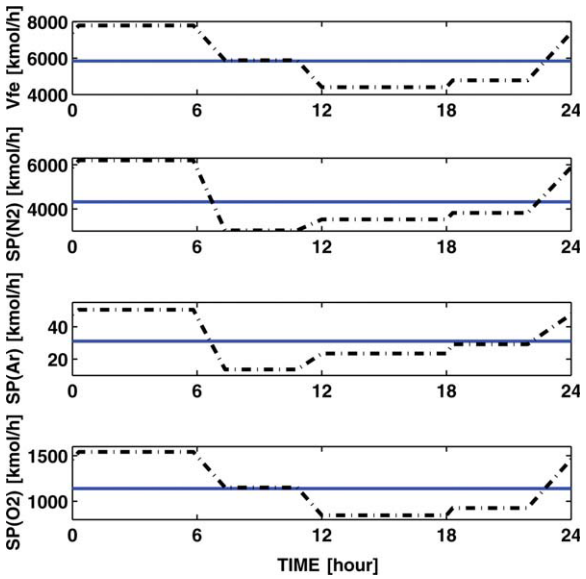

Figure 4. Profiles for total air feed flow rate (Vfe) and production rates of each component (SP).

The solid lines represent the optimal values when operating conditions are forced to be constant, and the dashed lines represent the multiperiod solution. [Color figures can be viewed in the online, which is available at wileyonlinelibrary.com]

where $S^{\mathrm{P}}_{i,n}$ are the production rates in the nth period, as defined by the process model. $\overline{S}^{\mathrm{P}}_{i,n}$ are the production rates at the front boundary of the period ($t = T^{\mathrm{M}}_n$) given by,

$$\bar{S}^{\mathrm{P}}_{i,n} = S^{\mathrm{P}}_{i,n} - \left(\frac{S^{\mathrm{P}}_{i,n} - S^{\mathrm{P}}_{i,n-1}}{T^{\mathrm{F}}_n - T^{\mathrm{S}}_{n-1}}\right)\left(T^{\mathrm{F}}_n - T^{\mathrm{M}}_n\right), i \in \mathcal{P}, \quad n \in (2,3,4) \tag{30}$$

$$\bar{S}^{\mathrm{P}}_{i,1} = S^{\mathrm{P}}_{i,1} - \left(\frac{S^{\mathrm{P}}_{i,1} - S^{\mathrm{P}}_{i,4}}{24 + T^{\mathrm{F}}_1 - T^{\mathrm{S}}_4}\right)\left(T^{\mathrm{F}}_1 - T^{\mathrm{M}}_1\right), i \in \mathcal{P}. \tag{31}$$

To satisfy the product demands, product storage is included and the following constraints can be added,

$$I_{i,n-1} + \Phi^{\mathrm{L}}_{i,n} - I_{i,n} = D_{i,n}, i \in \mathcal{P}, n \in (2,3,4) \tag{32}$$

$$I_{i,4} + \Phi^{\mathrm{L}}_{i,1} - I_{i,1} = D_{i,1}, i \in \mathcal{P}, \tag{33}$$

where $I_{i,n}$ is the inventory level of the ith product in the nth period. $D_{i,n}$ are the product demand amounts of the ith product in the nth period. The variables, $\Phi^{\mathrm{L}}_{i,n}$, are the total amounts of each product liquefied at the nth period.

Optimal Operating Strategy: Constant Product Demands

In this section, we present a case study assuming that the product demands are known and constant throughout day so that the only variation is in peak and off-peak power pricing. The revenues generated by supplying product to customers are the same in each period, and the objective minimizes operating costs associated with power usage as given by,

$$\min \mathbb{O} = \sum_{n=1}^{4} P^{\mathrm{E}}_n \left(W^{\mathrm{C}}_n + W^{\mathrm{L}}_n\right) \tag{34}$$

where P^{E}_n is the price of electricity in the nth period. Note that other costs associated with delivery and transportation could be included in the above function; however, they do not directly affect the optimal operating strategy of the process.

Two different operating strategies are compared. In the first strategy, the operating conditions are assumed to be constant over the entire day. The second strategy is the multiperiod formulation where the operating conditions are allowed to change. This case study demonstrates that transitioning among different operating conditions can reduce the operating costs compared with constant operation.

These two cases are formulated using the AMPL modeling language[13] and solved using IPOPT.[14] It is assumed that the constant product demands in each period for nitrogen, argon, and oxygen are 25920 ol, 187 ol, and 6843 kmol, respectively. Five main manipulated variables are selected for optimization: the feed air stream of the HPC, U_1, the feed air stream of the LPC, U_2, the reflux flow from the HPC to the LPC, U_3, the waste nitrogen stream, U_4, and the side withdrawal from the LPC to the CAC-1, U_5.

Figure 4 shows the profiles of the air feed flow and production rates for both the constant case (solid line) and the multiperiod case (dashed line). As expected, the desired feed flowrate (and hence the load on the plant) is lowest when the price of electricity is the highest and vice versa. The optimal transition times over the four periods are (5:49-7:21, 10:49-12:00, 18:00-18:18, and 21:54-0:19). Given the high cost of electricity in the third period, the optimal transition times are such that the lowest feed flow rate is utilized over this entire period. The optimization has effectively determined, not only the operating conditions within each period, but also the specific time to start and end each transition.

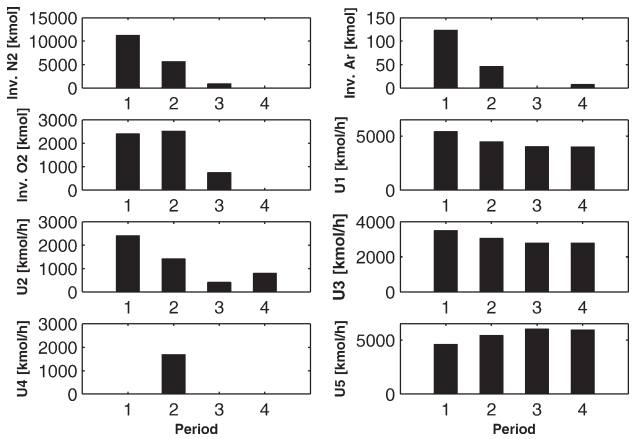

Figure 5. Optimal results for inventory levels (inv) and manipulated variables (U) in the multiperiod case.

The variation in these times demonstrates the importance of including these degrees of freedom instead of specifying fixed transition points. For the multiperiod case, Figure 5 shows the inventory levels at the end of each period and the values for the manipulated variables. In this case study, the product demands were kept constant. Therefore, to meet these demands throughout the day, the optimal inventory levels for each of the three products are highest before their lowest production rate. Comparing these two test cases, there is an overall savings of 5.11% in the total operating costs if we allow multiperiod operation instead of operating at a fixed steady state. This represents a significant savings for an air separation plant where operating costs can be very high. Furthermore, the possible savings are a direct function of the gap between high and low electricity prices. There is potential for increased savings in cases where variability in electricity pricing is higher.

Optimal Operating Strategies for Uncertain Product Demands

In addition to variability in power prices, in certain gas product markets air separation plants may need to switch operating conditions to satisfy variable product demands from different customers. Furthermore, the actual demand for specific products may not be known a priori. In this section, we focus on a multiperiod problem formulation that considers optimal operating plans for air separation processes with variable (but known) electricity prices and uncertain product demands.

Uncertainty in product demands has a direct effect on expected revenue and, hence, profits. Furthermore, contractual obligations may place constraints on the amount of demand that must be met. As described by Li et al[8] and Nahmais et al,[9] we use the loss function to evaluate the expected revenue and, assuming a Type 2 service level, formulate probabilistic fill-rate constraints on customer demands. In this section, we describe the necessary changes to the multiperiod formulation and show how the solution is affected by increasing demand uncertainty.

In any given time period, the actual amount of product sold to customers is the minimum of the customer demand and the available product (production plus available inventory). Therefore, the objective function includes the expected revenue from sale of product i in time period n, and the operating costs, as given by,

$$\max \mathbb{P} = \sum_{n=1}^{4} \sum_{i \in \mathcal{P}} \mathrm{Rev}_{i,n} - \sum_{n=1}^{4} P_n^{\mathrm{E}} \left(W_n^{\mathrm{C}} + W_n^{\mathrm{L}} \right), \tag{35}$$

where the expected revenue is,

$$\mathrm{Rev}_{i,n} = \mathbf{E}_{\hat{D}_{i,n}} \left[P_i^{\mathrm{P}} \cdot min\left(\hat{S}_{i,n}, \hat{D}_{i,n} \right) \right], i \in \mathcal{P}, n \in (1,2,3,4). \tag{36}$$

The available supply of product i in period n is given by,

$$\hat{S}_{i,n} = \begin{cases} \Phi_{i,n}^{\mathrm{L}} + I_{i,n-1} & n \in (2,3,4) \\ \Phi_{i,1}^{\mathrm{L}} + I_{i,4} & n = 1. \end{cases} \tag{37}$$

The parameters, P_i^{P}, are the known prices for the ith product, which are assumed constant throughout the day. Here, we assume that the prices of nitrogen, argon, and oxygen products are \$0.113/L, \$0.286/L, and \$0.176/L, respectively.[15,16] The variables, $\hat{D}_{i,n}$, are the uncertain demands of the ith product in the nth period.

Defining $\rho\left(\hat{D}_{i,n}\right)$ as the density function of the uncertain demand, the revenue can be written as,

$$\begin{aligned} \mathrm{Rev}_{i,n} &= P_i^{\mathrm{P}} \int_0^{+\infty} \rho\left(\hat{D}_{i,n}\right) \cdot \mathbf{min}\left(\hat{S}_{i,n}, \hat{D}_{i,n}\right) d\hat{D}_{i,n} \\ &= P_i^{\mathrm{P}} \left(\int_0^{\hat{S}_{i,n}} \rho\left(\hat{D}_{i,n}\right) \hat{D}_{i,n} d\hat{D}_{i,n} + \int_{\hat{S}_{i,n}}^{+\infty} \rho\left(\hat{D}_{i,n}\right) \hat{S}_{i,n} d\hat{D}_{i,n} \right) \\ &= P_i^{\mathrm{P}} \left(\theta_{i,n} - \int_{\hat{S}_{i,n}}^{+\infty} \left(\hat{D}_{i,n} - \hat{S}_{i,n}\right) \rho\left(\hat{D}_{i,n}\right) d\hat{D}_{i,n} \right), \\ & \qquad i \in \mathcal{P}, n \in (1,2,3,4) \end{aligned} \tag{38}$$

where the mean of the uncertain product demand, $\theta_{i,n}$, is equal to $\int_0^{+\infty} \rho\left(\hat{D}_{i,n}\right) \hat{D}_{i,n} d\hat{D}_{i,n}$. The expression, $\int_{\hat{S}_{i,n}}^{+\infty} \rho\left(\hat{D}_{i,n}\right) \left(\hat{D}_{i,n} - \hat{S}_{i,n}\right) d\hat{D}_{i,n}$ is called the loss function. If the demands are assumed normally distributed with the mean, $\theta_{i,n}$, and the deviation, $\sigma_{i,n}$, the loss function can be expressed by

$$\begin{aligned} & \int_{\hat{S}_{i,n}}^{+\infty} \rho\left(\hat{D}_{i,n}\right) \left(\hat{D}_{i,n} - \hat{S}_{i,n}\right) d\hat{D}_{i,n} \\ &= \sigma_{i,n} \int_{\frac{\hat{S}_{i,n} - \theta_{i,n}}{\sigma_{i,n}}}^{\infty} \left(\tau - \frac{\hat{S}_{i,n} - \theta_{i,n}}{\sigma_{i,n}} \right) \frac{1}{\sqrt{2\pi}} e^{\frac{-\tau^2}{2}} d\tau \\ &= \sigma_{i,n} \mathcal{L}\left(\frac{\hat{S}_{i,n} - \theta_{i,n}}{\sigma_{i,n}} \right), i \in \mathcal{P}, n \in (1,2,3,4), \end{aligned} \tag{39}$$

and finally the expected revenue is written as,

$$Rev_{i,n} = P_i^{P} \left[\theta_{i,n} - \sigma_{i,n} \mathcal{L}\left(\frac{\hat{S}_{i,n} - \theta_{i,n}}{\sigma_{i,n}} \right) \right], i \in \mathcal{P}, n \in (1,2,3,4). \tag{40}$$

Here, $\mathcal{L}(\cdot)$ is defined as the standardized loss function. From Eq. 40, the expected amount of product i sold to customers in period n is $\theta_{i,n} - \sigma_{i,n} \mathcal{L}\left(\frac{\hat{S}_{i,n} - \theta_{i,n}}{\sigma_{i,n}} \right)$. The numerical integration of the standardized loss function can be expressed by piecewise polynomial functions.[8]

Since we are now considering the expected value for product sales, the inventories are expected values as well, as defined by,

$$I_{i,n} = \hat{S}_{i,n} - \left[\theta_{i,n} - \sigma_{i,n} \mathcal{L}\left(\frac{\hat{S}_{i,n} - \theta_{i,n}}{\sigma_{i,n}} \right) \right], i \in \mathcal{P}, n \in (1,2,3,4). \tag{41}$$

In addition to the impact on expected profit, uncertain demands may have an impact on customer satisfaction levels if the plant is not able to deliver the desired product

Table 2. Mean Product Demands and Fill-Rate Over Four the Time Periods

	Period 1	2	3	4
θ_{N2}, kmol	20736	25920	33696	25920
θ_{Ar}, kmol	150	187	243	187
θ_{O2}, kmol	5474	6843	8896	6843
$\beta_{N2,n}$,	60%	70%	90%	70%
$\beta_{Ar,n}$,	60%	70%	90%	70%
$\beta_{O2,n}$,	60%	70%	90%	70%

amounts. Two types of customer service levels have been described,[8,9] where customer satisfaction is measured by whether or not actual customer demands are met in a given interval. The Type 1 service levels (called confidence levels) have been adopted in the application of chance-constrained programming,[8,17] and can be written as

$$Pr_{\varphi}\{\Psi^{i}(\varphi_i) \geq 0\} \geq \alpha_i \tag{42}$$

where α is the confidence level decided by managers. This type of formulation ensures that customer demand will be satisfied with a given probability; however, it does not consider the magnitude of the deficit when the demand is not met.

In this article, we consider Type 2 service levels. The Type 2 service level (also called the fill-rate) measures the expected fraction of demand that can be met by a plant. The Type 2 service level is typically more consistent with actual contracts.[9] Here, the expected sales of product i is constrained to be at least some fraction of the expected demand,[8] as given by,

$$\theta_{i,n} - \sigma_{i,n}\mathcal{L}\left(\frac{\hat{S}_{i,n} - \theta_{i,n}}{\sigma_{i,n}}\right) \geq \beta_{i,n}\theta_{i,n} \tag{43}$$

where β is the fill-rate specified in the contract.

To handle demand uncertainty, the original multiperiod formulation is modified as follows. The fill-rate constraints (43) are added, the original inventory constraints (32) and (33) are replaced with (41), and the objective function is changed to that described in Eq. 35. Assuming a known distribution for the product demands, this probabilistic formulation can be solved to maximize expected profits while maintaining contractual obligations.

Here, we assume that the product demands are normally distributed with known mean and standard deviation obtained from statistical analysis of historical data. In this section, we demonstrate that the multiperiod formulation can be solved efficiently while considering this demand uncertainty. Table 2 shows the values for the mean demands and the fill-rates. In the next three case studies, the standard deviation in the uncertain demand of argon is varied from 15 to 18% while nitrogen and oxygen are kept constant at 20%, as seen in Table 3.

Table 3 also shows the optimal objective value for each of these case studies. There is almost no difference in the optimal objective value between case study 3 and 4. This implies that the fill-rate constraint for argon is not active and that the process is able to meet the customer satisfaction constraints with optimal operating conditions based on profit considerations alone. As seen in case study 5, increasing the standard deviation of argon from 17.5 to 18% causes a reduction in the optimal objective value. Here, the fill-rate constraint for argon in period 3 becomes active and profits suffer because of the need to meet customer satisfaction levels. Solving different case studies and examining the values of the constraint multipliers corresponding to the fill-rate constraints allows managers to effectively evaluation the contractual obligations and their impact (at least locally) on profits. In addition to this analysis, the formulation also provides an optimal multiperiod operating strategy, including operating conditions and transition times.

In this example, if we increase the standard deviation on the argon demand to 20%, the optimization problem becomes infeasible, indicating that the current plant is not able to meet the customer satisfaction constraints with this level of uncertainty. This is important information for managers, showing the challenges associated with increased uncertainty. At this point, management has few choices to deal with the increased uncertainty. They can try to find additional resources or seek to increase facility capacity in order to meet customer requirements. Management may also choose to negotiate different contracts, guaranteeing lower uncertainty in product demands or reducing required fill-rates. Detailed case studies addressing the effect of varying fill-rates have been discussed in our previous work[7]. Of course, selection of values for fill-rates needs to account for multiple product interactions. In this particular case study, reducing the fill-rate for argon in period 3 from 90 to 80% makes the problem feasible again, with an optimal objective value of $\$5.30 \cdot 10^5$.

This case study illustrates the potential tradeoffs between profit and customer satisfaction levels in the face of uncertainty and variable power pricing. More importantly, this multiperiod formulation gives engineers an effective tool to analyze these tradeoffs using a rigorous model of their facility.

Conclusions and Future Work

Because of external pressures like variable power prices and product demands, it can be profitable to vary operating conditions regularily, instead of operating at a fixed steady state. This article presents a multiperiod formulation to determine optimal operating strategies for an energy-intensive air separation plant. In particular, the results demonstrate that a rigorous nonlinear model can be used in a mathematical programming formulation addressing both variability in inputs and uncertainty in desired product demands. The formulation contains a rigorous mathematical model for the highly-coupled air separation process including four coupled distillation columns, heat exchanges, compressors, and liquifiers. Transitions were not assumed to be instantaneous, but

Table 3. Results for Different Standard Deviations in Argon Demand

	σ_{N2}/θ_{N2}	σ_{O2}/θ_{O2}	σ_{Ar}/θ_{Ar}	Optimal Obj.
Case 3	20%	20%	15%	$\$5.42 \cdot 10^5$
Case 4	20%	20%	17.5%	$\$5.42 \cdot 10^5$
Case 5	20%	20%	18%	$\$5.39 \cdot 10^5$

Table 4. Symbols

Symbol	Definition
j	Index of each tray
F_j^{V}	Vapor molar feed flows
F_j^{L}	Liquid molar feed flows
S_j^{V}	Vapor molar side flows
S_j^{L}	Liquid molar side flows
V_j	Vapor flow rates
L_j	Liquid flow rates
$y_{i,j}$	Vapor compositions
$x_{i,j}$	Liquid compositions
$z_{i,j}^{\mathrm{V}}$	Vapor compositions of feed flows
$z_{i,j}^{\mathrm{L}}$	Liquid compositions of feed flows
H_j^{FV}	Vapor enthalpies of feed flows
H_j^{FL}	Liquid enthalpies of feed flows
$\underline{H}_{i,j}^{\mathrm{FV}}$	Vapor enthalpies of pure components in the feed flow
$\underline{H}_{i,j}^{\mathrm{FL}}$	Liquid enthalpies of pure components in the feed flow
$\underline{H}_{i,j}^{\mathrm{V}}$	Vapor enthalpies of pure components in each tray
$\underline{H}_{i,j}^{\mathrm{L}}$	Liquid enthalpies of pure components in each tray
ΔH_{mix}	Enthalpies of mixing
$a_{i,k}$	Margules constants
Q_1	Energy transferred within the combined condenser/reboiler
Q_2	Energy transferred in the condenser of the CAC-1
Q_3	Energy transferred in the reboiler of the CAC-2
UA_1, UA_2, UA_3	Heat transfer coefficients in the condenser/reboiler
T_1^{HPC}	Temperature in the first tray of the HPC
T_{70}^{LPC}	Temperature in the last tray of the LPC
$T_1^{\mathrm{CAC-1}}$	Temperature of the first tray of the CAC
$T_{O_2-\mathrm{rich}}^{\mathrm{HPC}}$	Temperature of the oxygen-rich liquid stream from the bottom of the HPC
T_{10}^{HPC}	Temperature in the 10th tray of the HPC
$T_{41}^{\mathrm{CAC-2}}$	Temperature in the last tray of the CAC-2
κ	Adiabatic index number of gas
η_1	Compression efficiency
Φ_n^{F}	Total amount of air feed flow into the air separation system
$P_{\mathrm{in}}^{\mathrm{C}}$	Entering flow pressures of the compressor
$P_{\mathrm{out}}^{\mathrm{C}}$	Exiting flow pressures of the compressor
ΔV_{loss}	Flow loss ratio of the air compressor
η_2	Liquifier efficiency
$V_{i,n}^{\mathrm{L}}$	Liquefied product flows
$\Delta H_{i,n}^{\mathrm{L}}$	Liquefied product enthalpy changes
T^{M}	Time period changes
V_n^{A}	Air feed flow rate
$\overline{V}_n^{\mathrm{A}}$	Air feed flow rate at the start of a period
b_n	Transition slope
T_n^{S}	Start time of transition
T_n^{F}	Final time of transition
$\Phi_{i,n}^{\mathrm{L}}$	Total amount of each liquefied product at the nth period
$S_{i,n}^{\mathrm{P}}$	Production rates in the nth period
$\overline{S}_{i,n}^{\mathrm{P}}$	Production rates at the front boundary of the period
$I_{i,n}$	Inventory level of the ith product in the nth period
$D_{i,n}$	Product demand amounts of the ith product in the nth period
$\Phi_{i,n}^{\mathrm{L}}$	Total amounts of each product liquefied at the nth period
P_n^{E}	Price of electricity in the nth period

(*Continued*)

Table 4. (Continued)

Symbol	Definition
U_1	Feed air stream of the HPC
U_2	Feed air stream of the LPC
U_3	Reflux flow from the HPC to the LPC
U_4	Waste nitrogen stream
U_5	Side withdrawal from the LPC to the CAC-1
P_i^{P}	Known prices for the ith product
$\hat{D}_{i,n}$	Uncertain demands of the ith product in the nth period
$\rho(\hat{D}_{i,n})$	Density function of the uncertain demand
$\theta_{i,n}$	Mean of the uncertain product demand
$\sigma_{i,n}$	Deviation of the uncertain product demand
$\mathcal{L}(\cdot)$	Standardized loss function
β	Contract specified fill-rate

rather are assumed to be proportional to the required load change. Furthermore, the optimization variables include the operating conditions in each period as well as the start time for each of the transitions. Uncertainty is addressed through use of the loss function in both the objective function and in fill-rate constraints on supplied product. The loss function is used to express the expected value of the plant revenue, and provide a means to constrain customer satisfaction levels. Because uncertainty exists on the process outputs only, this approach allows a probabilistic treatment without the need for a multiscenario formulation.

This formulation is used in several case studies to illustrate the effectiveness of the approach. As described in the first two case studies, the formulation can easily and rigorously determine the potential for improved profits comparing the optimal steady state case with the optimal multiperiod operating strategy. In the case study presented, multiperiod operation resulted in a 5% reduction in operating costs, however, increased savings are possible when power pricing variability is higher. The final four case studies consider uncertainty in product demands and, in particular, increased uncertainty in argon demand. These case studies illustrate that the approach can effectively handle this uncertainty, while providing management with valuable information regarding the tradeoff between profit and contractual obligations. It can be used to provide effective bounds on the level of uncertainty that can feasibly be addressed by the plant. Furthermore, since the formulation uses a rigorous process model, the approach provides facility specific operating strategies.

The multiperiod formulation presented in this article uses a rigorous model of the air separation plant, however, modern nonlinear programming tools can obtain solutions very efficiently. The six case studies in the article all contained over 3500 variables and solved in under ten seconds on a 3.2 GHz Intel Xeon processor.

Future work will include extending this formulation to include a rigorous dynamic model of the air separation process. We have previously developed a rigorous dynamic optimization formulation for optimal load changes in air separation processes.[18] This formulation can be extended to include variable power pricing and uncertainty in product demands. Furthermore, control strategies (e.g. model predictive control) could be included in the formulation to realistically describe the required switching time. Parallel nonlinear programming algorithms may be necessary to ensure efficient solution of these large-scale problems.

Acknowledgments

The authors gratefully acknowledge financial support provided by the Mary Kay O'Connor Process Safety Center at Texas A&M University.

Literature Cited

1. Bian S, Henson M, Belanger P, Megan L. Nonlinear state estimation and model predictive control of nitrogen purification columns. *Ind Eng Chem Res*. 2005;44:153–167.
2. Karwan MH, Keblis M. Operations planning with real time pricing of a primary input. *Comput Operation Res*. 2007;34:848–867.
3. Energy information association. Manufacturing energy consumption survey. Available at: http://www.eia.doe.gov/emeu/mecs/mecs2002/data02/shelltables.html. 2002.
4. Zhu Y, Legg S, Laird CD. Optimal design of cryogenic air separation columns under uncertainty. *Comput Chem Eng*. 2010;34:1377–1384.
5. Ierapetritou MG, Wu D, Vin J, Sweeney, PG, Chigirinskiy, M. Cost minimization in an energy-intensive plant using mathematical programming approaches. *Ind Eng Chem Res*. 2002;41:25262–5277.
6. Miller J, Luyben W, Blouin S. Economic incentive for intermittent operation of air separation plants with variable power costs. *Ind Eng Chem Res*. 2008;47:1132–1139.
7. Zhu Y, Legg S, Laird CD. Optimal operation of cryogenic air separation columns with demand uncertainty and contractual obligations. *Chem Eng Sci*.
8. Li W, Hui C, Li P, Li A. Refinery planning under uncertainty. *Ind Eng Chem Res*. 2004;43:6742–6755.
9. Nahmias S. *Production and Operation Analysis*, 5th ed. Singapore: McGraw-Hill Press, 2005.
10. Harmens A. Vapour-liquid equilibrium N2-Ar-O2 for lower argon concentrations. *Cryogenics*. 1970;6:406.
11. Baukal CE. *Oxygen-enhanced combustion*. New York: CRC Press, 1998.
12. Li, H. *Technology of oxygen production*, 1st ed. Beijing: Metallurgy Industry Press, 1996.
13. Fourer R, Gay DM, Kernighan BW. *AMPL: A modeling language for mathematical programming*, 2nd ed. New York: Duxbury Press, 2002.
14. Wächter A, Biegler LT. On the implementation of an interior-point filter line-search algorithm for large-scale nonlinear programming. *Math Programing*. 2006;106:25–57.
15. Salerno LJ, Gaby J, Johnson R, Kittel P, Marqurdt ED. *Terrestrial applications of zero-boil-off cryogen storage*, (Cryocoolers, edited by R. G. Ross, Jr.) 11:809–816.
16. Kerry FG. *Industrial gas handbook: gas separation and purification*. New York: Taylor & Francis Press, 2006.
17. Li P, Arellano HG, Wonzy G. Chance constrained programming approach to process optimization under uncertainty. *Comput Chem Eng*. 2008;32:25–45.
18. Zhu Y, Laird CD. *A parallel algorithm for structured nonlinear programming*. In: Proceedings, Foundations of Computer-Aided Process Operations, 5th ed. Boston, June 29–July 2, 2008, 345–348.

Manuscript received Mar. 29, 2010, revision received July 13, 2010, and final revision received Oct. 5, 2010.